CR6-interacting factor 1 is a key regulator in Aß-induced mitochondrial disruption and pathogenesis of Alzheimer's disease

OPEN

Cell Death and Differentiation (2015) 22, 959–973

www.nature.com/cdd

CR6-interacting factor 1 is a key regulator in Aβ-induced mitochondrial disruption and pathogenesis of Alzheimer's disease

J Byun[1,6], SM Son[1,6], M-Y Cha[1], M Shong[2], YJ Hwang[3], Y Kim[3], H Ryu[3,4], M Moon[5], K-S Kim[5] and I Mook-Jung[*,1]

Mitochondrial dysfunction, often characterized by massive fission and other morphological abnormalities, is a well-known risk factor for Alzheimer's disease (AD). One causative mechanism underlying AD-associated mitochondrial dysfunction is thought to be amyloid-β (Aβ), yet the pathways between Aβ and mitochondrial dysfunction remain elusive. In this study, we report that CR6-interacting factor 1 (Crif1), a mitochondrial inner membrane protein, is a key player in Aβ-induced mitochondrial dysfunction. Specifically, we found that Crif1 levels were downregulated in the pathological regions of Tg6799 mice brains, wherein overexpressed Aβ undergoes self-aggregation. Downregulation of Crif1 was similarly observed in human AD brains as well as in SH-SY5Y cells treated with Aβ. In addition, knockdown of Crif1, using RNA interference, induced mitochondrial dysfunction with phenotypes similar to those observed in Aβ-treated cells. Conversely, Crif1 overexpression prevented Aβ-induced mitochondrial dysfunction and cell death. Finally, we show that Aβ-induced downregulation of Crif1 is mediated by enhanced reactive oxygen species (ROS) and ROS-dependent sumoylation of the transcription factor specificity protein 1 (Sp1). These results identify the ROS-Sp1-Crif1 pathway to be a new mechanism underlying Aβ-induced mitochondrial dysfunction and suggest that ROS-mediated downregulation of Crif1 is a crucial event in AD pathology. We propose that Crif1 may serve as a novel therapeutic target in the treatment of AD.
Cell Death and Differentiation (2015) **22,** 959–973; doi:10.1038/cdd.2014.184; published online 7 November 2014

Alzheimer's disease (AD) is the most common and rapidly growing dementia among the aged population worldwide. Representative pathologies of AD include the accumulation of amyloid β (Aβ) plaques, the formation of neurofibrillary tangles, and massive neuronal loss in the brain.[1,2] Although many studies have focused on the amyloid-β precursor protein (APP) or Aβ as a therapeutic target, the mechanisms by which Aβ aggravates AD are not yet fully known. Many possible scenarios have been suggested based on several lines of evidence related to mitochondrial dysfunction, oxidative stress, cerebrovascular damage, and inflammation.[3] Among these hypotheses, abnormal mitochondrial function in AD is known as a primary causative factor in AD pathogenesis.[4,5] In this study, therefore, we focused on a possible mechanism of mitochondrial dysfunction in the progression of AD.

In mammals, mitochondria are vital organelles participating in energy production, calcium buffering, signal cascade, and cell survival.[6] Two oxidative metabolic processes, the citric acid cycle and fatty acid β-oxidation, take place in the mitochondrial matrix, whereas the oxidative phosphorylation (OXPHOS in short) system or respiratory chain is embedded in the mitochondrial inner membrane (MIM). Mitochondria quality control is regulated by fusion and fission processes, which are tightly regulated by several proteins, such as mitofusins (Mfn1 and Mfn2), optic atrophy type 1 (OPA1), mitochondrial fission 1 protein (Fis1), and dynamin-related protein 1 (DRP1).[7] Mitochondrial dynamics are important for mitochondrial morphology and function. If the balance between fusion and fission is disrupted, mitochondrial morphology is disrupted, and thus, mitochondrial function is severely impaired.[8] Owing to their high-energy metabolic rate, neurons are highly dependent on mitochondria, and therefore, neurons are more vulnerable to mitochondrial dysfunction than other cell types.[5] Previous studies revealed that impaired mitochondrial dynamics are associated with neurodegenerative diseases, including Parkinson's disease (PD) and

[1]Department of Biochemistry and Biomedical Sciences, Seoul National University College of Medicine, Seoul, Korea; [2]Research Center for Endocrine and Metabolic Diseases, Chungnam National University School of Medicine, Daejeon, Korea; [3]Center for Neuro-Medicine, Brain Science Institute, KIST, Seoul, Korea; [4]Department of Neurology and Pathology, Boston University School of Medicine, Boston, MA, USA and [5]Department of Psychiatry, McLean Hospital/Harvard Medical School, Belmont, MA, USA

*Corresponding author: I Mook-Jung, Department of Biochemistry and Biomedical Sciences, Seoul National University College of Medicine, 28 Yungun-dong, Seoul 110-799, Korea. Tel: +82 2 740 8245; Fax: +82 2 3672 7352; E-mail: inhee@snu.ac.kr

[6]These authors contributed equally to this work.

Abbreviations: AD, Alzheimer's disease; Aβ, amyloid beta; APP, amyloid beta precursor protein; Crif1, CR6-interacting factor 1; Crif1 KD cell, Crif1 knock-downed cell; Crif1 o/e cell, Crif1 overexpressed cell; Co-IP, co-immunoprecipitation; Calcein-AM, acetomethoxy derivate of Calcein; DAB, 3,3′-Diaminobenzidine; DPI, diphenyleneiodonium; EMSA, gel electrophoresis mobility shift assay; Fis1, mitochondrial fission 1 protein; GAPDH, glyceraldehyde 3-phosphate dehydrogenase; HD, Huntington's disease; HSP60, Heat-shock protein 60; MTT, 3-(4,5-dimethylthiazol-2-yl)-2,5-diphenyltetrazolium bromide; MIM, mitochondrial inner membrane; Mfn, mitofusins; NAC, N-acetylcysteine; NADPH, nicotine adenine diphosphate oxidase; OPA1, optic atrophy type 1; OXPHOS, oxidative phosphorylation; PD, Parkinson's disease; qRT-PCR, quantitative real-time PCR; ROS, reactive oxygen species; RuR, Ruthenium Red; Sp1, specificity protein 1; TUNEL, Terminal deoxynucleotidyl transferase dUTP nick end labeling; WB, western blotting; 3-MA, 3-methyladenine

Received 01.4.14; revised 25.8.14; accepted 25.9.14; Edited by L Scorrano; published online 07.11.14

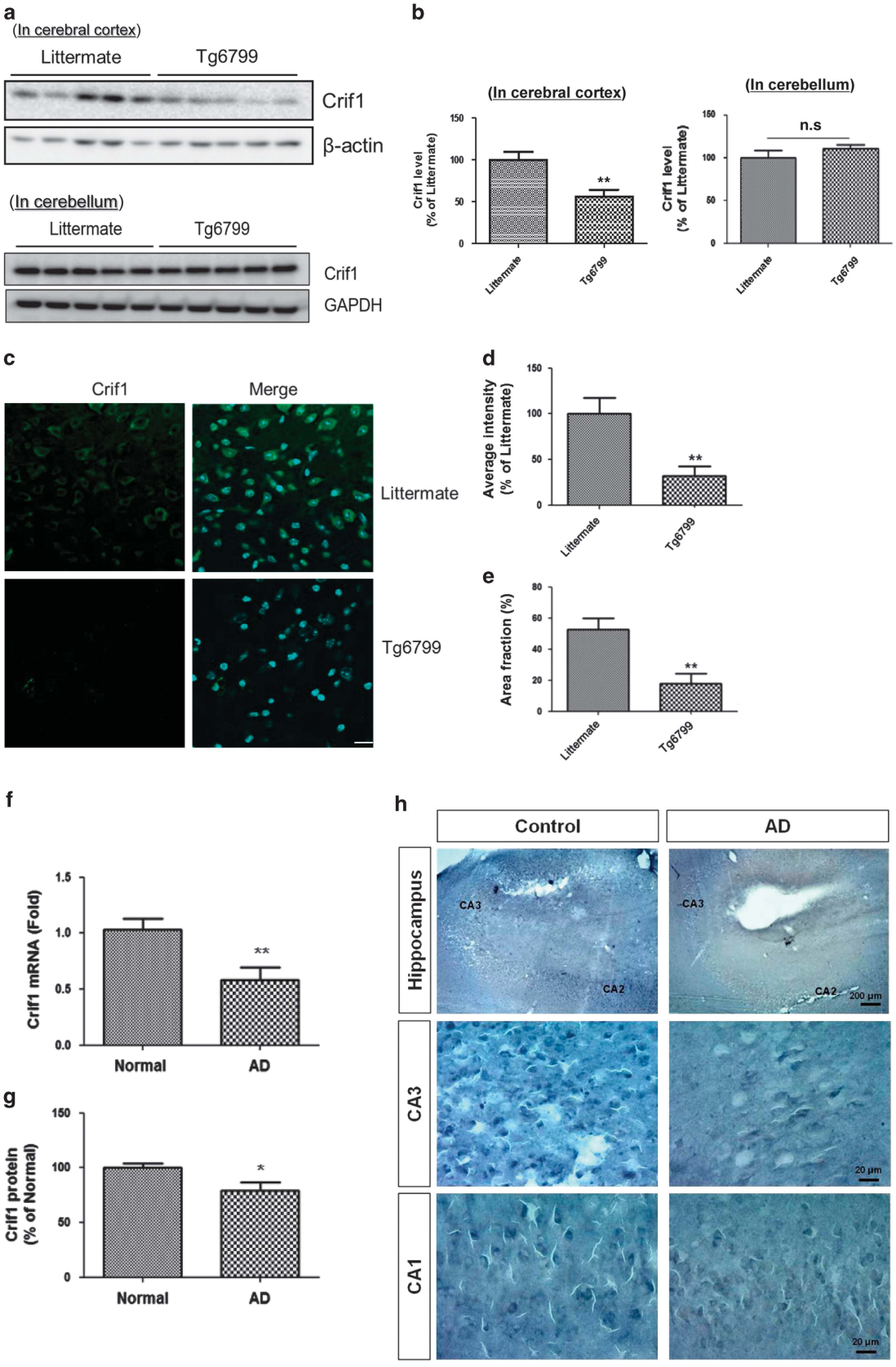
a
(In cerebral cortex)
Littermate
Tg6799
Crif1
β-actin
(In cerebellum)
Littermate
Tg6799
Crif1
GAPDH
b
(In cerebral cortex)
Crif1 level (% of Littermate)
150
100
50
0
**
Littermate
Tg6799
(In cerebellum)
Crif1 level (% of Littermate)
150
100
50
0
n.s
Littermate
Tg6799
c
Crif1
Merge
Littermate
Tg6799
d
Average intensity (% of Littermate)
150
100
50
0
**
Littermate
Tg6799
e
Area fraction (%)
80
60
40
20
0
**
Littermate
Tg6799
f
Crif1 mRNA (Fold)
1.5
1.0
0.5
0.0
**
Normal
AD
g
Crif1 protein (% of Normal)
150
100
50
0
*
Normal
AD
h
Control
AD
Hippocampus
CA3
CA2
200 μm
CA3
CA2
200 μm
CA3
20 μm
20 μm
CA1

Huntington's disease (HD).[9] As in other neurodegenerative diseases, mitochondrial fragmentation has also been observed in the brains of AD patients.[10] Furthermore, elevated oxidative stress levels were detected in the brains of AD patients.[11] In addition, reduced amounts of mitochondrial DNA, destructed mitochondrial cristae, and inner/outer mitochondrial membrane structure are also directly linked to the increased incidence of AD.[12] However, the molecular mechanisms underlying impaired mitochondrial dynamics and function in AD are unclear.

CR6-interacting factor 1 (Crif1), also known as GADD45-associated family protein, was first identified as a molecule that regulates cell cycle and growth.[13,14] Recently, some nuclear receptors, such as Nur77, STAT3, Elf3, and Nrf2, are also known to interact with Crif1.[15] In addition, Crif1 is important for the translation of mitochondrial OXPHOS subunits and their insertion into the MIM.[16] In this study, we investigated whether Crif1 has a role in AD pathogenesis, and found that Crif1 acts as a key player in Aβ–induced mitochondrial dysfunction. First, we found that the expression level of Crif1 was reduced in the brains of AD mouse models as well as in brain tissues from AD patients. Next, we investigated whether Aβ regulates Crif1 expression levels *in vitro*, and we found that Crif1 was decreased significantly in Aβ-treated SH-SY5Y cells compared with vehicle-treated cells. In addition, this process was mediated by elevated ROS levels via activation of NADPH oxidase. To examine the mechanism in detail, Aβ-induced ROS facilitated the reduced binding of the specificity protein 1 (Sp1) transcription factor on the promoter region of Crif1 by increasing the sumoylation of Sp1. Reduced Crif1 expression resulted in the disruption of mitochondrial morphology and its functions, which leads to massive cell death in AD brains. Finally, Crif1 overexpression (Crif1 o/e) rescued Aβ-induced mitochondrial alteration and neuronal cell death. These data suggest that the regulation of Crif1 could be explored as a therapeutic target for AD.

Results

Crif1 is decreased in the brains of AD patients and AD mouse models. To determine whether Crif1 expression is altered in the brains of AD mice, endogenous Crif1 levels in the frontal cortex, hippocampus, and cerebellum in 6-month-old Tg6799 mice were evaluated by western blot analysis (WB). Crif1 levels were reduced significantly in the frontal cortex, and the hippocampus of Tg6799 mice compared with non-transgenic littermate controls, respectively (Figures 1a and b and Supplementary Figures 1a and b). However, Crif1 levels in the cerebellum of Tg6799 mice were not different from those in littermate controls (Figures 1a and b), suggesting that Crif1 reduction occurs only in the pathological areas of AD. In addition, the expression of Crif1 was examined by immunohistochemistry using a specific antibody against Crif1. Both intensity and area fraction of Crif1 fluorescence signal in Tg6799 mouse brains were significantly decreased compared with those of littermate controls (Figures 1c–e). These results were also confirmed in brains of other AD model mice, such as the APP/PS1 mice (Supplementary Figure 1c). As PS1 mutations causing early-onset AD modulate protein expression by disrupting endoplasmic reticulum homeostasis,[17] to determine whether decreased Crif1 levels in Tg6799 and APP/PS1 mouse brains were caused by PS1 mutations, we measured Crif1 levels in the brains of 12-month-old Tg2576 mice that carry only the APP mutation (Supplementary Figure 1c). The levels of Crif1 were reduced in Tg2576 mice compared with non-transgenic littermate controls, indicating that Aβ pathology-bearing mice show a reduction of Crif1 expression regardless of mutant PS1 expression. To determine whether Crif1 level is also altered in brains of AD patients, quantitative real-time PCR (qRT-PCR) and WB analyses in the superior temporal cortex of human brains, showed a reduction in Crif1 mRNA and protein levels in AD patients, as much as 35% and 21%, respectively, compared with control brains (Figures 1f and g). In addition, immunohistochemical analysis of postmortem human brain sections, containing the hippocampus, CA3, and CA1 regions, revealed that the intensity of Crif1 3, 3'-diaminobenzidine (DAB) staining was decreased in AD patients (Figure 1h, Supplementary Table 1). Overall, these data indicate that Crif1 expression is reduced in pathological areas of AD brains.

Aβ_{1-42} affects Crif1 expression by modulating Crif1 mRNA. The above *in vivo* data showed reduced Crif1 levels in the pathological regions of AD (Figure 1 and Supplementary Figure 1), and APP mutation-bearing mouse models showed decreased Crif1 expression levels (Supplementary Figure 1b); thus, we determined whether Aβ, a major risk factor for AD, alters Crif1 expression. Exogenous Aβ_{1-42}, but not A$\beta_{42\text{-}1}$ (reverse form of A$\beta_{1\text{-}42}$), decreased endogenous Crif1 levels in SH-SY5Y cells in time- (Figure 2a) and dose-dependent manners (Figure 2b). Immunofluorescence experiments, using anti-Crif1 and anti-HSP60 antibodies, the latter a mitochondria indicator, showed that Aβ decreased intracellular Crif1 levels (Figure 2c). To examine whether Aβ-induced Crif1 reduction is cell specific, Aβ was applied to HT22 cells, the mouse hippocampal neurons. HT22 cells showed decreased Crif1 levels after Aβ treatment (Supplementary Figure 2a). To examine the mechanism of downregulation of Crif1 by Aβ in SH-SY5Y cells, we checked whether Crif1 is degraded by

Figure 1 Crif1 expression was decreased in the brains of mouse models of AD and AD patients. (**a** and **b**) WB analysis showed that Crif1 was decreased in the frontal cortex (not in the cerebellum) of 6-month-old Tg6799 mice ($n=5$ per group). Data are presented as mean percentage ± S.E.M. $^{**}P<0.01$, NS indicates no significant difference. (**c**–**e**) Representative micrographs showing immunohistochemistry in the frontal cortex of 6-month-old Tg6799 mice ($n=6$ per group). (**d** and **e**) Both the intensity (**d**) and area fraction (**e**) of the Crif1 signaling were significantly reduced. The fluorescent signals were captured by fluorescence microscopy and analyzed by Image J software. Data are presented as mean percentage ± S.E.M. $^{**}P<0.01$. Scale bar represents 20 μm. (**f** and **g**) qPCR analysis (**f**) and WB analysis (**g**) of brains from AD patients (AD) and controls (normal) revealed downregulation of Crif1 mRNA and protein expression in AD patients ($n=4$ per group), $^{*}P<0.05$; $^{**}P<0.01$. (**h**) Nickel-enhanced diaminobenzidine/peroxidase reaction showed decreased Crif1 signal in AD patients. Scale bars represent 200 μm (hippocampus) and 20 μm (CA1 and CA3), respectively

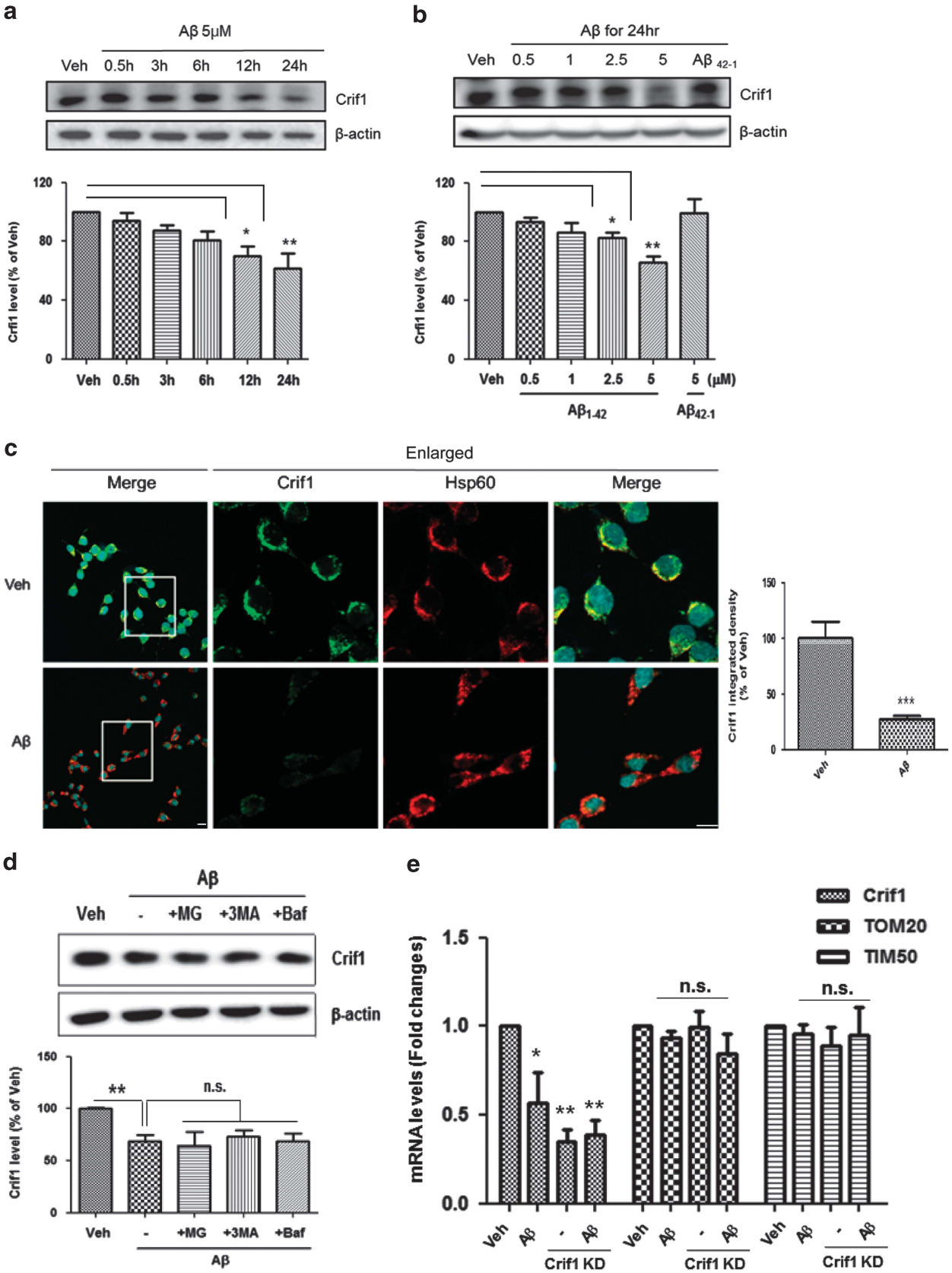
a
Aβ 5μM
Veh 0.5h 3h 6h 12h 24h
Crif1
β-actin
Crif1 level (% of Veh)
120
80
40
0
Veh 0.5h 3h 6h 12h 24h
b
Aβ for 24hr
Veh 0.5 1 2.5 5 Aβ 42-1
Crif1
β-actin
Crif1 level (% of Veh)
Veh 0.5 1 2.5 5 5 (μM)
Aβ1-42
Aβ42-1
c
Enlarged
Merge
Crif1
Hsp60
Merge
Veh
Aβ
Crif1 integrated density (% of Veh)
150
100
50
0
***
Veh
Aβ
d
Aβ
Veh - +MG +3MA +Baf
Crif1
β-actin
Crif1 level (% of Veh)
150
100
50
0
**
n.s.
Veh - +MG +3MA +Baf
Aβ
e
Crif1
TOM20
TIM50
mRNA levels (Fold changes)
1.5
1.0
0.5
0.0
*
**
**
n.s.
n.s.
Veh Aβ - Aβ
Crif1 KD
Veh Aβ - Aβ
Crif1 KD
Veh Aβ - Aβ
Crif1 KD

degradation pathways such as the proteasome and/or autophagy-lysosomal pathways. We found that MG132, a potent proteasome inhibitor,[18] and/or 3-methyladenine (3-MA) and bafilomycin, inhibitors of the autophagy-lysosomal system,[19] failed to rescue Aβ-induced Crif1 reduction (Figure 2d), suggesting that Aβ-mediated Crif1 regulation did not occur via protein degradation. Next, we checked for changes in the transcriptional levels of Crif1 after Aβ treatment by using qRT-PCR. We found that Aβ reduced Crif1 mRNA levels without reducing the mRNA levels of other mitochondrial proteins, such as TOM20 (translocase of outer mitochondrial membranes 20 kDa) and TIM50 (translocase of inner mitochondrial membrane 50 kDa), indicating that Aβ disturbs the transcriptional processing of Crif1 (Figure 2e). In addition, the reduction of Crif1 mRNA levels lasted for 24 h after Aβ treatment (Supplementary Figure 2b). These data indicate that Aβ induced the reduction of Crif1 levels at the transcriptional level.

Crif1 mRNA is downregulated by Aβ-induced ROS by facilitating sumoylation of the Sp1 transcription factor. Previous studies showed that Aβ increased ROS production via the activation of several pathways, and the increased ROS has been proposed to have a harmful role in AD pathogenesis.[3,5] To check the effect of ROS on Crif1 levels, treatment with H_2O_2 reduced Crif1 levels significantly (Figure 3a). To determine specifically whether Aβ-induced ROS generation reduced Crif1 levels, treatment with the ROS scavenger, N-acetylcysteine (NAC), could rescue Crif1 levels in Aβ-treated SH-SY5Y cells (Figure 3b), indicating that Crif1 levels are affected by ROS levels, which might be excessively increased by Aβ.[5] ROS are formed as byproducts of mitochondrial respiration or by the action of oxidases, including nicotine adenine diphosphate (NADPH) oxidase, and xanthine oxidase.[20] Because Aβ is known to accelerate ROS generation by activating NADPH oxidase,[21] and Aβ-induced Crif1 reduction is mediated by ROS, we examined whether NADPH oxidase mediates Aβ-induced Crfi1 regulation. When treatment of Aβ with apocynin and diphenyleneiodonium (DPI), well-known NADPH oxidase inhibitors,[22,23] was applied to SH-SY5Y cells, Crif1 levels showed an increase compared with Aβ-treated cells. These data indicate that Aβ-induced activation of NADPH oxidase generates ROS, thereby reducing Crif1 levels. Because Aβ-induced reduction of Crif1 expression levels is mediated by transcriptional regulation in Figure 2e, to further investigate the mechanisms of Crif1 reduction by Aβ, we used a software program to search for transcription factor-binding sites with the promoter region sequence of Crif1 (http://www.genetools.us/genomics/). Through the binding motif analysis, we identified several candidate transcription factors, including AML-1A, SRY, and Sp1. Among them, Sp1 is a ubiquitous transcription factor, and has been previously reported to be an ROS-sensitive transcription factor for other proteins.[24,25] To determine whether Sp1 binds to the Crif1 gene promoter region, gel electrophoresis mobility shift assay (EMSA) was performed (Figure 3d). There was a reduction in the moving distance in a non-denaturing gel because of the binding of Sp1 to the probe, the Crif1 gene promoter sequence (Figure 3d, arrowhead). We also found that 5 μM of Aβ treatment resulted in reduced binding between Sp1 and Crif1 promoter region by detecting a less intense signal on the gel (Figure 3d, arrowhead). According to previous studies, sumoylation of Sp1 blocks the cleavage for the negative regulatory domain of Sp1 and decreases Sp1-dependent transcription.[26] As increased ROS facilitates sumoylation of many proteins, and high ROS levels have been demonstrated in AD,[5,24,25] we tested the possibility that abnormal over-production of ROS in AD might cause sumoylation of Sp1, thereby decreasing Sp1-dependent transcription of Crif1. To determine whether Aβ increased sumoylation of Sp1, we performed co-immunoprecipitation (Co-IP) experiments with Sp1- and SUMO-1-specific antibodies. We found that Aβ enhanced the interaction between Sp1 and SUMO-1, which indicates that Aβ-induced Sp1 sumoylation (Figures 3e and f). To test the effects of Sp1 sumoylation on Crif1 levels, Sp1 wild type and Sp1 K16A, a sumoylation-deficient mutant of Sp1,[27] cDNAs were transfected to SH-SY5Y cells. When Aβ was applied to cells, Sp1 K16A mutant-transfected cells showed less decrease in Crif1 levels compared with Sp1 wild-type-transfected cells (Figure 3g). These data indicate that Aβ-induced reduction of Crif1 is mediated by sumoylation of Sp1, which negatively affects binding of Sp1 to the Crif1 gene promoter following gene expression.

Crif1 is crucial for maintaining mitochondrial morphology in SH-SY5Y cells. Previous studies have demonstrated the disruption of mitochondrial morphology and impaired mitochondrial function in AD.[28] Aβ seems to contribute to these phenomena, by inducing excessive mitochondrial fission and failure of the OXPHOS system.[29] Disrupted mitochondrial morphology was consistently observed in the cortex of Tg6799 mouse brains upon EM analyses (Figure 4a).

Figure 2 Aβ reduced Crif1 levels in SH-SY5Y cells through transcriptional regulation. (**a**) Crif1 levels were significantly reduced by Aβ (5 μM) in a time-dependent manner. Data were obtained from at least four replicates for each group ($N=4$ experiments). Data are presented as mean $\pm$ S.E.M. *$P<0.05$; **$P<0.01$ *versus* vehicle (dimethyl sulfoxide (DMSO))-treated cells. (**b**) Crif1 levels were significantly decreased by A$\beta_{1\text{-}42}$ (24 h), but not the reversed form of A$\beta_{1\text{-}42}$, in a dose-dependent manner. Data were obtained from at least four replicates for each group ($N=4$ experiments). Data are presented as mean $\pm$ S.E.M. *$P<0.05$, **$P<0.01$. β-Actin is used as a loading control in **a** and **b**. (**c**) Confocal images showing reduced Crif1 signal in mitochondria of SH-SY5Y cells treated with 2.5 μM Aβ for 24 h. Scale bar represents 10 μm. Quantification of Crif1 signal was analyzed using the Image J program. Data are represented as mean $\pm$ S.E.M. from three independent experiments. ***$P<0.001$. (**d**) Aβ-induced Crif1 reduction was not mediated by protein degradation pathway. MG132 (10 μM), 3-MA (2 mM), and bafilomycin (5 nM) were administered 1 h before Aβ treatment, and 24 h after incubation, WB was performed to measure Crif1 levels. β-Actin serves as a loading control. Representative images are shown. Data are represented as mean $\pm$ S.E.M. from three independent experiments. **$P<0.01$ *versus* vehicle-treated cells; NS *versus* Aβ-treated cells. (**e**) qRT-PCR analysis showed that Aβ decreased Crif1 mRNA levels in SH-SY5Y cells without affecting mRNA levels of other mitochondrial proteins such as TOM20 and TIM50. Reduced levels of Crif1 after siRNA transfection were detected by qRT-PCR. Data are represented as the mean $\pm$ S.E.M. from three independent experiments. *$P<0.05$, **$P<0.01$, *versus* vehicle-treated cells

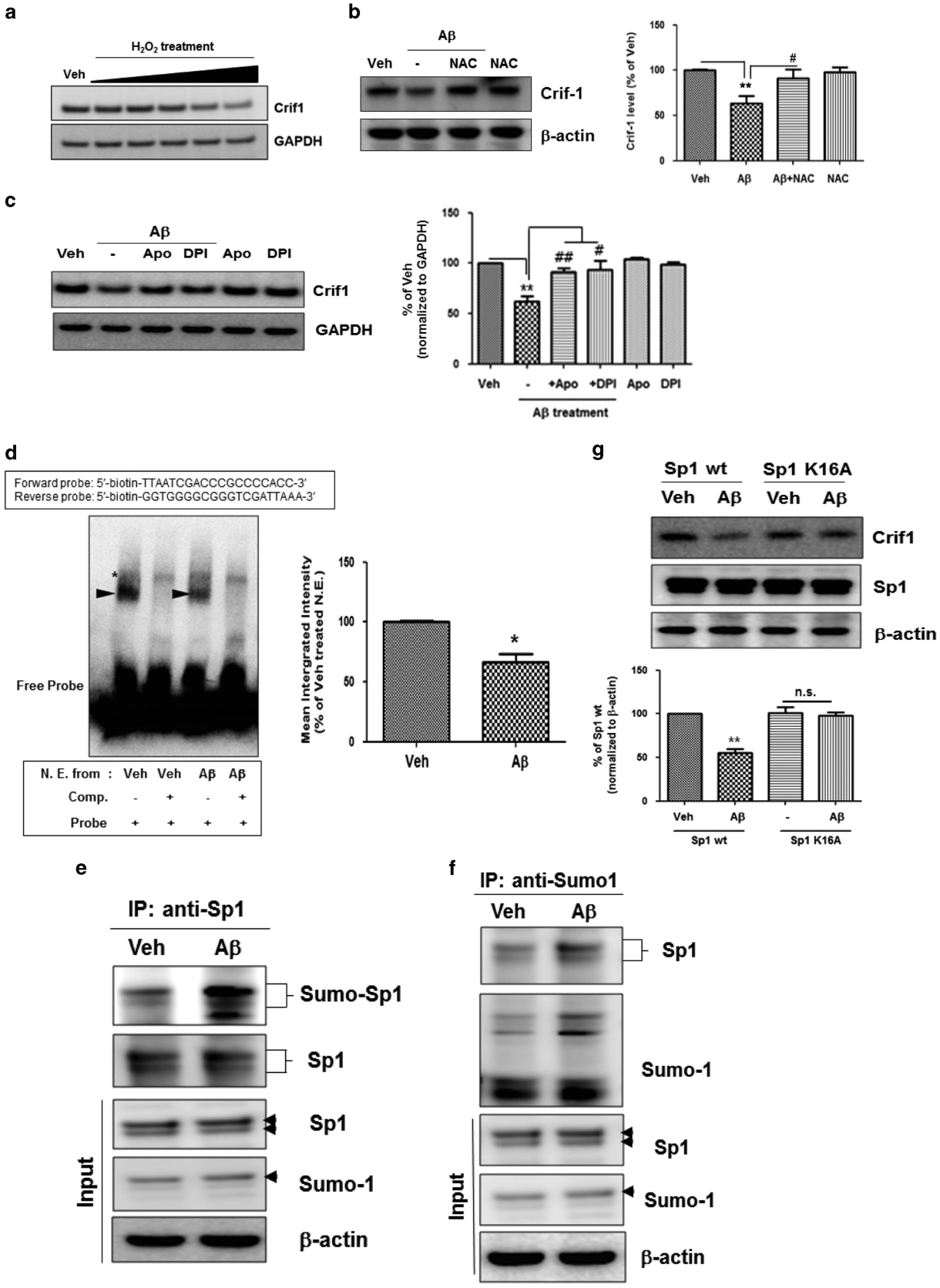
a
H_2O_2 treatment
Veh
Crif1
GAPDH
b
Aβ
Veh - NAC NAC
Crif-1
β-actin
Crif-1 level (% of Veh)
Veh Aβ Aβ+NAC NAC
c
Aβ
Veh - Apo DPI Apo DPI
Crif1
GAPDH
% of Veh (normalized to GAPDH)
Veh - +Apo +DPI Apo DPI
Aβ treatment
d
Forward probe: 5'-biotin-TTAATCGACCCGCCCCACC-3'
Reverse probe: 5'-biotin-GGTGGGGCGGGTCGATTAAA-3'
Free Probe
N. E. from : Veh Veh Aβ Aβ
Comp. - + - +
Probe + + + +
Mean Intergrated Intensity (% of Veh treated N.E.)
Veh Aβ
g
Sp1 wt Sp1 K16A
Veh Aβ Veh Aβ
Crif1
Sp1
β-actin
% of Sp1 wt (normalized to β-actin)
n.s.
Veh Aβ - Aβ
Sp1 wt Sp1 K16A
e
IP: anti-Sp1
Veh Aβ
Sumo-Sp1
Sp1
Input
Sp1
Sumo-1
β-actin
f
IP: anti-Sumo1
Veh Aβ
Sp1
Sumo-1
Input
Sp1
Sumo-1
β-actin

Because previous studies show that Crif1 has a critical role in maintaining mitochondrial function via the integration of OXPHOS polypeptides into the mitochondrial membrane,[16] and Crif1 is mainly located in mitochondria (Supplementary Figures S3a and b), we investigated whether reduced Crif1 expression causes the disruption of mitochondrial morphology. We transfected SH-SY5Y cells with Crif1 siRNA (Crif1 KD), and the expression of Crif1 was reduced by as much as about 60% in relation to the control siRNA-transfected group (Figure 2e and Supplementary Figure 4a). Using a Mito-DsRed-expressing SH-SY5Y cell line, we analyzed alterations in mitochondrial morphology in control siRNA (Veh), Aβ-treated control siRNA(Aβ), Crif1 siRNA (Crif1 KD), and Aβ-treated Crif1 siRNA-transfected cells (Crif1 KD+Aβ; Figures 4b and c). Consistent with previous studies, mitochondria were shortened (represented by aspect ratio) and more circular (represented by form factor) after treatment with 5 μM of Aβ (Figure 4c). Interestingly, Crif1 knockdown itself (Crif1 KD) could disrupt mitochondrial morphology resembling that of Aβ-treated control siRNA-transfected cells (Aβ; Figures 4b and c). In addition, Aβ-treated Crif1 KD cells (Crif1 KD+Aβ) did not show further mitochondrial disruption compared with Crif1 KD cells, indicating that reduced Crif1 levels are sufficient to disrupt the mitochondrial structure (Figures 4b and c). Furthermore, massive mitochondrial fission and loss of cristae were observed in Crif1 KD cells using EM analysis (Figure 4d). To determine whether Crif1 interacts with mitochondrial fission/fusion protein, Co-IP with Crif1 and fission/fusion protein-specific antibodies was performed. We found no interaction between Crif1 and mitochondrial fission/fusion proteins (Supplementary Figure 5). These data suggest that Crif1 is important for maintaining mitochondrial morphology and that Aβ-induced mitochondrial disruption is mediated by attenuating Crif1 levels.

Loss of endogenous Crif1 leads to severe defects in various mitochondrial functions in SH-SY5Y cells. We determined whether Crif1 regulates mitochondrial function as well as mitochondrial morphology under Aβ-treated conditions. When Crif1 siRNA was transfected into SH-SY5Y cells, the mitochondrial membrane potential (MMP) was significantly attenuated using JC-1 and TMRM assays (Figure 4e and Supplementary Figure 6a). In addition, Cirf1 KD cells showed decreased ATP levels by ATP-luciferase assays (Figure 4f). To check ROS generation, we used the dichloro-dihydrofluoresceindiacetate and MitoSOX assays, which showed increased ROS generation in Crif1 KD cells (Figure 4g, and Supplementary Figure 6b). Overall, these data indicate that downregulated Crif1 expression induced mitochondrial dysfunctions as shown in AD condition.

Overexpression of Crif1 rescues Aβ-induced disruption of mitochondrial morphology. To examine whether Crif1 is a key molecule for maintaining mitochondrial integrity, either scrambled or Crif1 cDNA was transfected into SH-SY5Y cells. When Aβ was administered to the cells, Crif1 overexpression (o/e) cells showed healthy mitochondria in terms of length and shape (Figures 5a and b). To further confirm the role of Crif1 in mitochondrial function, mitochondrial functions were evaluated after scrambled or Crif1 cDNA transfection followed by Aβ treatment. Decreased MMPs and ATP synthesis were not fully, but were significantly, rescued as much as 50% and 20% in Crif1 o/e cells after evaluation with JC-1 (Figure 5c) and ATP-luciferase assays (Figure 5d), respectively. Strikingly, Aβ-induced ROS generation was completely blocked by Crif1 o/e (Figures 5e and f). These data show that Aβ decreases Crif1 levels, and enhances ROS generation, causing impairment in mitochondrial functions. In summary, our data suggest that Crif1 levels are essential to maintain mitochondrial homeostasis and Aβ-induced mitochondrial disruption is mediated by decreased Crif1 expression.

Crif1 levels are important for Aβ-induced cell death in SH-SY5Y cells. Previous studies have demonstrated that mitochondrial dysfunction leads to cell death *via* intrinsic apoptotic pathways.[30] To determine whether the Aβ-induced decrease in Crif1 can influence cell viability, 3-(4,5-dimethylthiazol-2-yl)-2,5-diphenyltetrazolium bromide (MTT) and Calcein-AM assays were performed (Figures 6a and b). We found that Crif1 KD alone, as well as Aβ treatment, caused significant cell death. Interestingly, overexpression of Crif1 significantly increased cell viability of Aβ-treated conditions (Figures 6c and d). To confirm the role of Crif1 on Aβ-induced cell death, TUNEL (TdT-mediated dUTP Nick-End Labeling) assays were performed (Figure 6e). Consistent with the results of MTT and

Figure 3 Aβ-induced ROS decreased the transcription of Crif1 gene by facilitating sumoylation of Sp1. (**a**) Treatment with H_2O_2-reduced Crif1 levels. 10–750 μM of H_2O_2 were administered for 6 h into SH-SY5Y cells, and then WB was performed to measure Crif1 levels. GAPDH is used as a loading control. Representative images are shown. (**b**) Treatment with a ROS scavenger (NAC; 1 mM) rescued Aβ-induced Crif1 downregulation. β-Actin is used as a loading control. Representative images are shown. Data are represented as mean $\pm$ S.E.M. from three independent experiments. $^{**}P<0.01$ *versus* vehicle-treated cells; $^{\#}P<0.05$ *versus* Aβ-treated cells. (**c**) Inhibition of NADPH oxidase rescued Aβ-induced Crif1 reduction. Apo (apocynin; 10 μM) or DPI (10 μM) was administered to vehicle- or Aβ-treated cells, and then WB was performed. Representative images are shown. Data are represented as mean $\pm$ S.E.M. from three independent experiments ($N=3$ experiments). $^{**}P<0.01$ *versus* vehicle-treated cells. $^{\#}P<0.05$, $^{\#\#}P<0.01$ *versus* Aβ-treated cells. (**d**) EMSA analysis showed that Aβ (5 μM, 24 h treatment) decreased the binding of Sp1 on the promoter region of Crif1. Asterisk (*) represents the nonspecific band, whereas the black arrowhead (protein-DNA probe complex) represents specific bands. NE indicates 'nuclear extracts', Comp indicates 'competition probe', and free probe indicates 'non-binding probe'. The intensity of the protein-probe complex was analyzed using Image J software. $^{*}P<0.05$. Representative images are shown ($N=2$ experiments). (**e**, **f**) Co-immunoprecipitation (Co-IP) analysis showed that sumoylation of Sp1 by SUMO-1 was enhanced after treatment with Aβ. The left panel (**e**) shows the increased Sp1-Sumo1 interaction in Aβ-treated cells, and the right panel (**f**) shows the increased Sp1 sumoylation in Aβ-treated cells using an anti-Sumo1 antibody. The lower panel ('Input') shows a WB of Sp1 and Sumo1, with β-actin as a loading control. Representative images are shown ($N=3$ experiments). (**g**) Sumoylation-deficient mutant form of Sp1 (Sp1 K16A) shows less reduction in Crif1 levels by Aβ compared with Sp1 wild-type (wt)-transfected cells. β-Actin as a loading control. Representative images are shown. Data are represented as mean $\pm$ S.E.M. from five independent experiments ($N=5$ experiments). $^{**}P<0.01$.*versus* vehicle-treated Sp1 wt-transfected cells

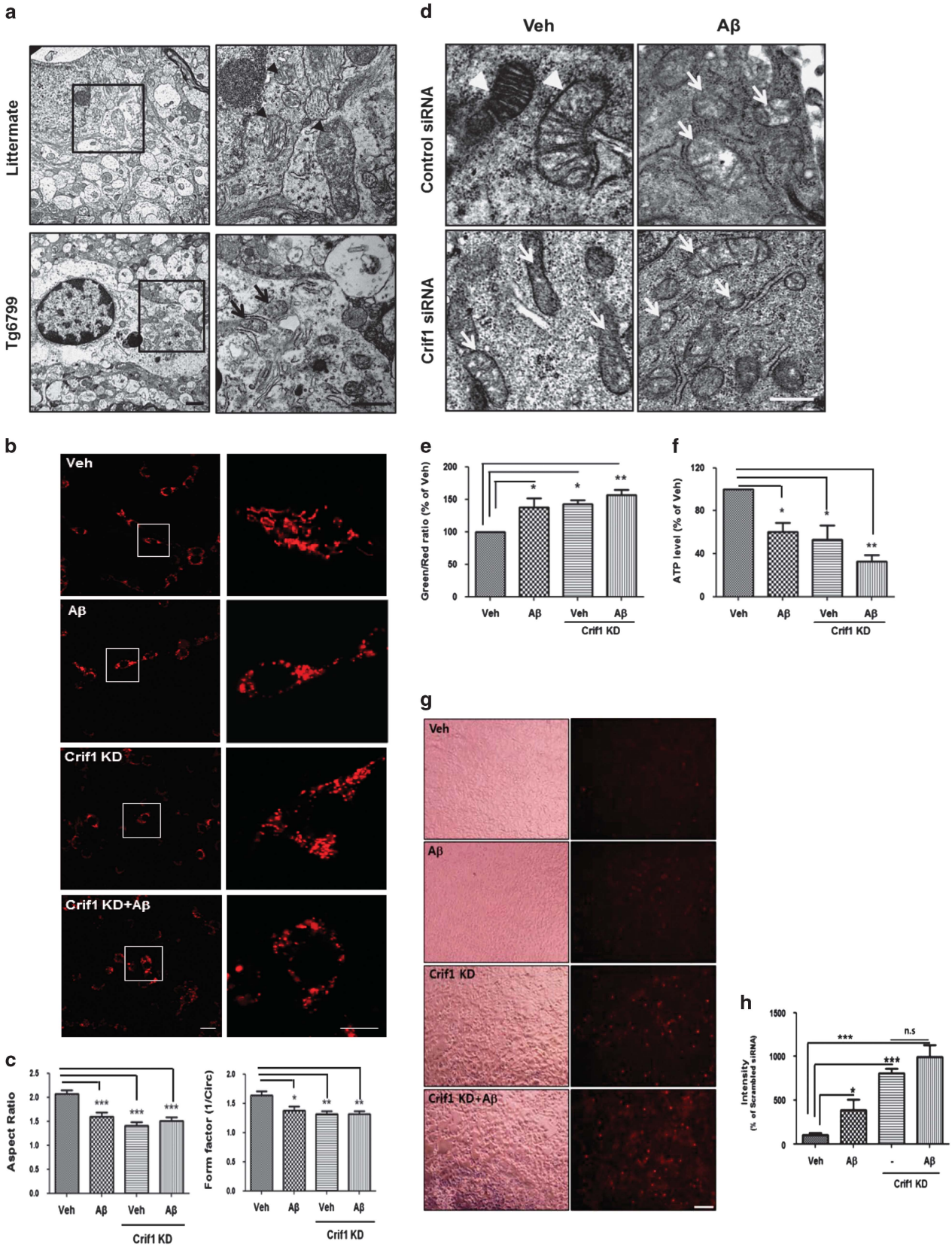
a
Littermate
Tg6799
d
Veh
Aβ
Control siRNA
Crif1 siRNA
b
Veh
Aβ
Crif1 KD
Crif1 KD+Aβ
e
Green/Red ratio (% of Veh)
Veh
Aβ
Veh
Aβ
Crif1 KD
f
ATP level (% of Veh)
Veh
Aβ
Veh
Aβ
Crif1 KD
g
Veh
Aβ
Crif1 KD
Crif1 KD+Aβ
c
Aspect Ratio
Veh
Aβ
Veh
Aβ
Crif1 KD
Form factor (1/Circ)
Veh
Aβ
Veh
Aβ
Crif1 KD
h
Intensity
(% of Scrambled siRNA)
n.s
Veh
Aβ
-
Aβ
Crif1 KD

Calcein-AM assays, o/e of Crif1 diminished Aβ-induced cell death. These data indicate that Crif1 levels are crucial for cell survival in the presence of Aβ.

Discussion

Although many studies have reported that Aβ induces severe mitochondrial dysfunction, which is believed to have a central role in AD pathogenesis,[12,28–32] how Aβ affects mitochondrial impairment is not yet fully understood. Previous findings demonstrated that several MIM structural proteins contribute to the maintenance of mitochondrial morphology, including cristae structures.[33–35] In a recent report, it was shown that Crif1 is important for maintaining mitochondrial function, and alterations in Crif1 levels cause severe mitochondrial dysfunction.[16] However, there were no data regarding the role of Crif1 in the brain and its relationship to pathological conditions. Here, we demonstrate the role of Crif1 in the brain and its regulation, particularly in the pathological condition of AD. This study provides *in vitro* and *in vivo* evidence that shows that reduced Crif1 levels, mediated by Aβ, cause mitochondrial defects, resulting in cell death (Figure 7). Recently, Crif1 was reported to be important for maintaining mitochondrial function by aiding the insertion of OXPHOS subunits and stabilizing the MIM integrity.[16] In our imaging data, using super-resolution microscopy, we confirmed that Crif1 is mainly located in MIM (Supplementary Figure 3); thus, the reduction in Crif1 levels might affect the stability of the OXPHOS system in MIM and the energy production required for cell survival. Furthermore, reduced Crif1 expression in AD brains would contribute to AD pathology by impairing the OXPHOS system and mitochondrial functions.

There is increasing evidence that ROS accelerate the progression of AD pathology during the early period of the disease.[36,37] However, the precise role of ROS in Aβ-induced neuronal loss has not yet been unraveled. In an effort to identify signaling molecules underlying the role of Crif1 in AD pathogenesis, we also found that Aβ-induced downregulation of Crif1, requires increased levels of ROS. These results were extended to an additional mechanism that ROS-dependent sumoylation of the Sp1 transcription factor has a role in Aβ-induced downregulation of Crif1 expression. Until now, there was no known transcription factor regulating the expression levels of Crif1, and we first identified that the ROS-sensitive transcription factor Sp1, regulates Crif1 levels directly after Aβ treatment. Previous studies showed that sumoylation of Sp1 attenuates protein stability and decreases the Sp1-dependent transcription,[26] whereas oxidative stress regulates Sp1 activity.[38] In addition, Sp1 dysregulation has been reported in AD brains,[39] suggesting that dysregulation of Sp1, by excessive ROS, might contribute to AD progression. In this study, we showed that Aβ increased Sp1 sumoylation by using Co-IP, indicating that Aβ might reduce Crif1 expression through increased Sp1 sumoylation (Figures 3e and f). Data obtained using a sumoylation-deficient mutant form of Sp1 confirmed these results (Figure 3g). In addition, co-treatment of Aβ with NADPH oxidase inhibitors (apocynin and DPI) rescued Aβ-induced Crif1 reduction in SH-SY5Y cells, suggesting that Aβ activates NADPH oxidase, resulting in ROS generation (Figure 3c). Previous reports showed that Aβ could induce pathological insults, including an increase in intracellular Ca^{2+}, inflammation, and endoplasmic reticulum stress, as well as ROS generation.[3,5,40] We also examined whether treatment with a Ca^{2+} chelator or chemical chaperone could block Aβ-induced Crif1 reduction. However, these blockers could not reverse the decrease in Crif1 levels (data not shown). These data indicate that Aβ induced down-regulation of Crif1 by elevating ROS level. It is well known that *in vivo* ROS levels are enhanced in vulnerable regions that exhibit AD pathology, such as the cortex and the hippocampus. Xie *et al.* reported that oxidative stress was more dramatic in neurites near plaques, and rapid cell death by amyloid plaque-mediated oxidative stress was shown in AD brains.[41] In previous studies, no plaques are shown in the cerebellum of AD brains,[42,43] so ROS-induced Crif1 reduction is mainly demonstrated in the cortex and the hippocampus (Figure 1 and Supplementary Figure 1), but not in the cerebellum (Figure 1a). Further studies on the Crif1 levels in many other neurodegenerative diseases, including PD and HD that are associated with increased ROS levels, should be investigated.

Our data showed that the dysregulation in mitochondrial dynamics (such as abnormal mitochondrial fission) mediated by Crif1 KD and/or the treatment with Aβ, induced mitochondrial dysfunction, resulting in cell death (Figure 4). However, in Figures 5 and 6, there is only a slight rescue in MMP and ATP production by overexpression of Crif1, yet almost we see a complete reversal of ROS production and apoptosis. There is an explanation for the results; in previous studies, Aβ is known

Figure 4 Crif1 knockdown (KD) disrupted mitochondrial morphology and impaired mitochondrial function. (**a**) Massive mitochondrial fission and loss (indicated by arrows) occurred in the frontal cortex of 6-month-old Tg6799 mice, whereas healthy filamentous mitochondria (indicated by arrowheads) were observed in age-matched littermate controls. The right panels show figures under higher magnification. Scale bar represents 2 μm (left panels) and 1 μm (right panels). (**b** and **c**) Crif1 KD induced increased mitochondrial fission (**b**). Mito-DsRed-expressing SH-SY5Y cells were transfected with control siRNA or Crif1 siRNA, and then treated with vehicle or Aβ for 12 h. The images were obtained by a confocal microscope, and the right panels show figures under higher magnification. (**c**) Mitochondrial morphology was analyzed using the Image J program (200 cells for each group). Mitochondria in Crif1 KD cells were shorter (represented by the aspect ratio) and had a more circular shape (represented by the form factor) in comparison to control siRNA-transfected cells. Data are represented as the mean $\pm$ S.E.M. from three independent experiments. $^{*}P<0.05$, $^{**}P<0.01$, $^{***}P<0.001$ *versus* vehicle-treated control siRNA-transfected cells. Scale bars represent 10 μm. (**d**) EM analysis revealed disrupted mitochondrial morphology in Crif1 KD cells similar to Aβ-treated cells. Arrowheads indicate intact and healthy mitochondria, whereas arrows point to disrupted mitochondria. Scale bar represents 1 μm. (**e**) The MMP was measured by JC-1 assay. Data presented as mean $\pm$ S.E.M. of three experiments ($N=3$ experiments). $^{*}P<0.05$, $^{**}P<0.01$ *versus* vehicle-treated control siRNA-transfected cells. (**f**) ATP generation in Crif1 KD cells was determined by ATP-luciferase assay. Crif1 KD cells show impaired ATP production. Data presented as mean $\pm$ S.E.M. from three experiments ($N=3$ experiments). $^{*}P<0.05$, $^{**}P<0.01$ *versus* vehicle-treated control siRNA-transfected cells. (**g** and **h**) ROS generation in Crif1 KD cells was determined by MitoSOX staining. (**g**) Left panel shows phase contrast imaging and right panel shows the fluorescence of MitoSOX dye representing production of mitochondrial superoxide. (**h**) Quantification data of **g** are presented here. Crif1 KD cells show massive ROS generation in mitochondria. Scale bar represents 50 μm. Data are represented as mean $\pm$ S.E.M. from three to five independent experiments. $^{*}P<0.05$, $^{***}P<0.001$ *versus* vehicle-treated control siRNA-transfected cells

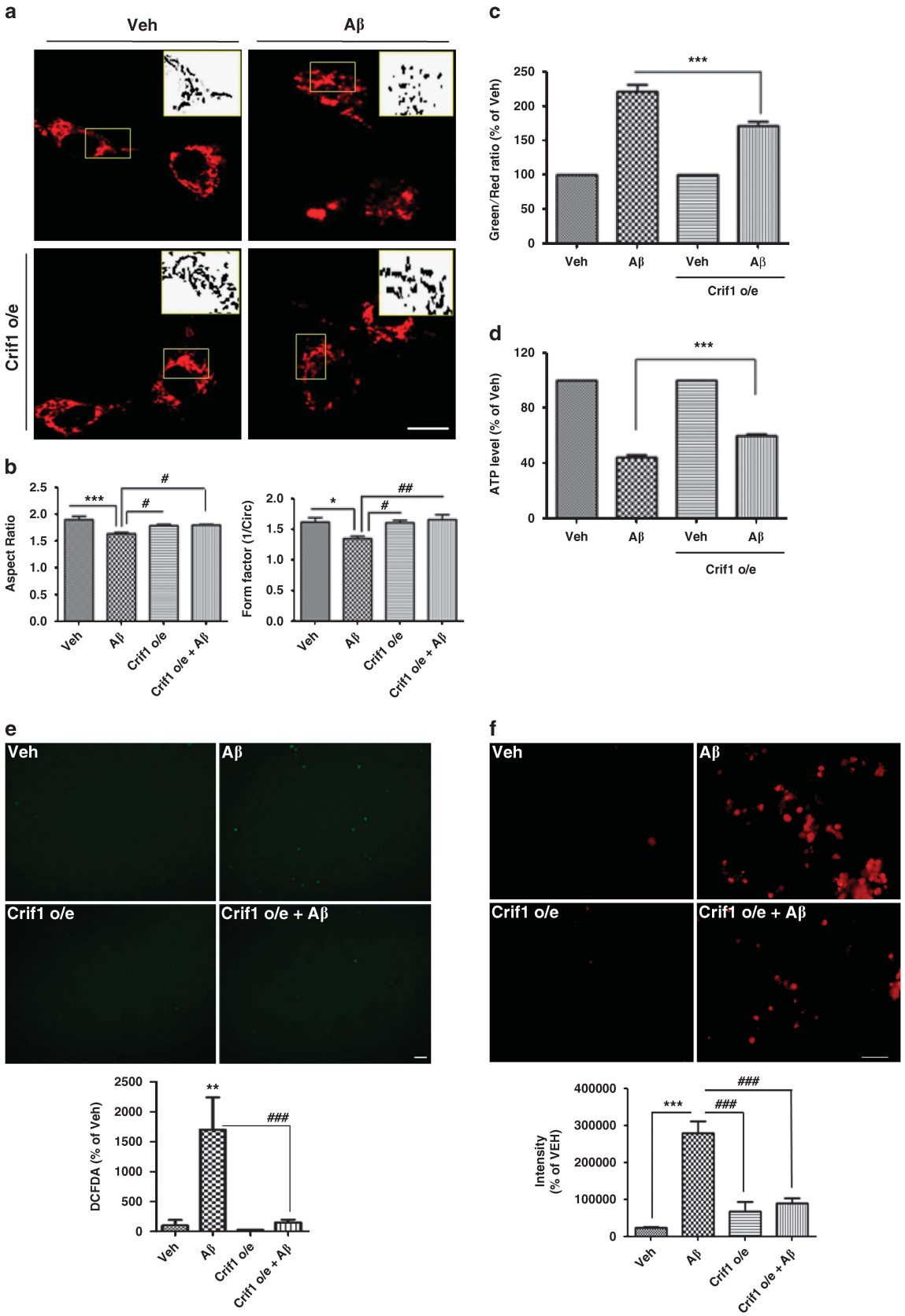
a
Veh
Aβ
Crif1 o/e
b
Aspect Ratio
Form factor (1/Circ)
Veh
Aβ
Crif1 o/e
Crif1 o/e + Aβ
c
Green/Red ratio (% of Veh)
Crif1 o/e
d
ATP level (% of Veh)
Crif1 o/e
e
DCFDA (% of Veh)
f
Intensity (% of VEH)

to interact with ATP synthase and cyclophilin D in the mitochondria,[44,45] and then results in decreased ATP production and the opening of the mitochondrial permeability transition pore. Because overexpression of Crif1 cannot block Aβ binding to its interacting partners, ATP levels and MMP might be partially, but significantly, rescued in Crif1-overexpressing cells. However, partially restored ATP, MMP, and inhibition of ROS might be enough to maintain cell survival as shown in Figures 6c–e.

Previous studies indicated that Aβ can enter the cells,[46] and mediate excitotoxicity by enhancing Ca^{2+} influx, which eventually leads to cell death.[47] Aβ has been found to induce mitochondrial Ca^{2+} overload through a mitochondrial Ca^{2+} uniporter (MCU). To determine whether Aβ-induced mitochondrial Ca^{2+} overload, induced mitochondria abnormalities and cell death, Ruthenium red (RuR), a nonspecific inhibitor of the MCU, and Ru360, a highly specific inhibitor of the MCU,[48] were administered to SH-SY5Y cells, and then MTT and Calcein-AM assays were performed. We found that treatment with MCU inhibitors (RuR and Ru360) along with Aβ failed to rescue Aβ-induced mitochondrial dysfunction and cell death (Supplementary Figures 7a and b). This result indicates that MCU-dependent Ca^{2+} influx into mitochondria, have no role in Aβ-induced mitochondrial dysfunction. Treatment with a ROS scavenger rescued Aβ-induced mitochondrial dysfunction and cell death. Our data indicate that Aβ-induced mitochondrial dysfunction and cell death are mainly mediated by ROS (Supplementary Figures 7a and b).

There are important MIM proteins that regulate mitochondrial morphology, including chchd3, mitofilin, ATP synthase, and prohibitin.[33–35,49,50] Ablation of these proteins is known to cause the disruption of mitochondrial morphology as well as severe mitochondrial dysfunction,[33,34,51] which was also observed in Crif1 KD MEF cells.[16] Massive neurodegeneration and hyper-phosphorylated tau were observed in prohibitin-deficient neurons in the forebrain of *phb2*^{nko} mice, implying that disruption of mitochondrial morphology by loss of MIM proteins is closely related to the development of AD pathology.[35] Thus far, there have been no detailed reports suggesting a close relationship between other MIM proteins and AD. Therefore, it is highly likely that dysregulation of these proteins in AD might induce mitochondrial dysfunction, and their role in AD should be further investigated in future studies.

Collectively, our results identify the ROS-Sp1-Crif1 pathway to be a new mechanism underlying Aβ-induced mitochondrial dysfunction and suggest that ROS-mediated downregulation of Crif1 is a crucial event in AD pathology (Figure 7). To investigate the relationship between other transcription factors besides Sp1, and Crif1 levels, inhibitors for several other transcription factors, including AP-1 and NF-κB, were administered together with Aβ into cells, and we found that these inhibitors did not block the reduction of Crif1 levels by Aβ (data not shown). Therefore, we hypothesize that the ROS-Sp1-Crif1 pathway regulates Aβ-induced mitochondrial dysfunction, which is a crucial event in AD pathology (Figure 7).

Materials and Methods

Animals and human brain samples. We used three different types of AD model mice: Tg2576 mice (expressing the APP Swedish mutation),[52] APP/PS1 mice (expressing Swedish APP and Presenilin1 delta exon 9 mutations),[53] and Tg6799 mice.[54] The Tg6799 mice (formerly JAX Stock No. 008730) overexpress both mutant human APP695 form along with the Swedish (K670N, M671L), Florida (I716V), and London (V717I) familial AD (FAD) mutations and human PS1 harboring two FAD mutations, M146L and L286V. All mice were purchased from Jackson Laboratories (Bar Harbor, ME, USA), and the animals maintained in Seoul National University's mouse facility. All experiments were approved by the Institute of Laboratory Animal Resources of Seoul National University. Human brain tissues for WB and qRT-PCR were obtained from Boston University, Boston, MA, USA, and postmortem tissue blocks, containing the hippocampal formation from AD patients (Braak V-VI) and healthy control donors for immunohistochemistry, were obtained from the Harvard Brain Tissue Resource Center, Belmont, MA, USA (see Supplementary Table 1 for additional information of human brain tissues).

Cell culture, transfection, and drug treatment. SH-SY5Y, a human neuroblastoma cell line, and HT22, an immortalized mouse hippocampal neuronal cell line, were cultured as previously described.[55] Cells were transfected with cDNA for Crif1 (gifted from Dr. Shong (Chungnam University, Korea)), Sp1 (hMU003598; provided from Korea Human Gene Bank, Medical Genomics Research Center, KRIBB, Korea), Sp1 K16A or Mito-DsRed using Lipofectamine and Plus reagents (Invitrogen, Carlsbad, CA, USA) and Crif1 siRNA (Santa Cruz Biotechnology, Santa Cruz, CA, USA) using RNAiMax reagents (Invitrogen) for 48 h according to the manufacturer's instructions. Cells were grown to 60% confluency and treated with vehicle (dimethyl sulfoxide) or A$\beta_{1\text{-}42}$ (American Peptide, Sunnyvale, CA, USA), A$\beta_{42\text{-}1}$ (Bachem, Bubendorf, Switzerland) and various reagents; MG132 (10 μM; M7449, Sigma-Aldrich, St. Louis, MO, USA), 3-MA (2 mM; M9281, Sigma-Aldrich), bafilomycin (5 nM; B1793, Sigma-Aldrich), NAC (1 mM; A7250, Sigma-Aldrich), apocynin (10 μM; A10809, Sigma-Aldrich), DPI (10 μM; D2926, Sigma-Aldrich), and H_2O_2 (216763, Sigma-Aldrich).

Western blotting. Harvested cell pellets and mouse brain tissues were prepared as previously described.[56] The antibodies used for WB were: anti-Crif1 (sc-134882), TOM20 (sc-17764), TOM40 (sc-11414), Drp1 (sc-32898), Fis1 (sc-98900), Mfn1 (sc-50330), and OPA1 (sc-30573) antibodies from Santa Cruz Biotechnology (1 : 500 for WB); anti-TIM50 (ab23938; 1 : 1000); GAPDH (ab9485; 1 : 3000)antibodies from Abcam; anti-Sp1 antibody (07–645) from Millipore (Billerica, MA, USA; 1 : 1000); anti-Sumo-1 (4930); HSP60(4870) antibodies from Cell Signaling Technology (Beverly, MA, USA; 1 : 1000 for WB; 1 : 200 for IP); anti-β-actin antibody from Sigma-Aldrich (1 : 3000). Immunoreactive bands were photographed and quantified on an LAS-3000 with Multi Gauge (Fuji Film Inc., Tokyo, Japan).

Mitochondrial morphology analysis. Mitochondrial morphology was investigated using Mito-DsRed-transfected SH-SY5Y cells. Briefly, 5 μM of Aβ was administered to the cells for 12 h before live-cell imaging or staining process.

Figure 5 Crif1 overexpression restored Aβ-induced mitochondrial dysfunction in SH-SY5Y cells. (**a** and **b**) Mock vector or Crif1 cDNA-transfected (Crif1 o/e) Mito-DsRed-expressed cells were treated with vehicle or 5 μM Aβ for 12 h. In small boxes, enlarged images were converted to 8-bit format to analyze mitochondrial morphology using the Image J program. Crif1 o/e recovered the increased mitochondrial fission by Aβ in terms of shape (form factor (**b**)) and length (aspect ratio (**b**)). Scale bar represents 10 μm. Data presented as mean ± S.E.M. from three experiments (200 cells for each group). *$P<0.05$, ***$P<0.001$ *versus* vehicle-treated mock-transfected cells. $^{\#}P<0.05$, $^{\#\#}P<0.01$ *versus* Aβ-treated mock-transfected cells. (**c**) The MMP was measured by JC-1 assay. Data presented as mean ± S.E.M. of four experiments. ***$P<0.001$ *versus* Aβ-treated mock vector-transfected cells. (**d**) ATP generation in Crif1 o/e cells was determined by ATP-luciferase assay. Data presented as mean ± S.E.M. from three experiments. ***$P<0.001$ *versus* Aβ-treated mock vector-transfected cells. (**e** and **f**) ROS generation in Crif1 o/e cells was determined by dichloro-dihydrofluoresceindiacetate (DCFDA; **e**) and MitoSOX (**f**) staining. Scale bar represents 10 μm (e) or 20 μm (**f**). Data are represented as the mean ± S.E.M. of five independent experiments. **$P<0.01$, ***$P<0.001$ *versus* vehicle-treated mock vector-transfected cells; $^{\#\#\#}P<0.001$ *versus* Aβ-treated mock vector-transfected cells

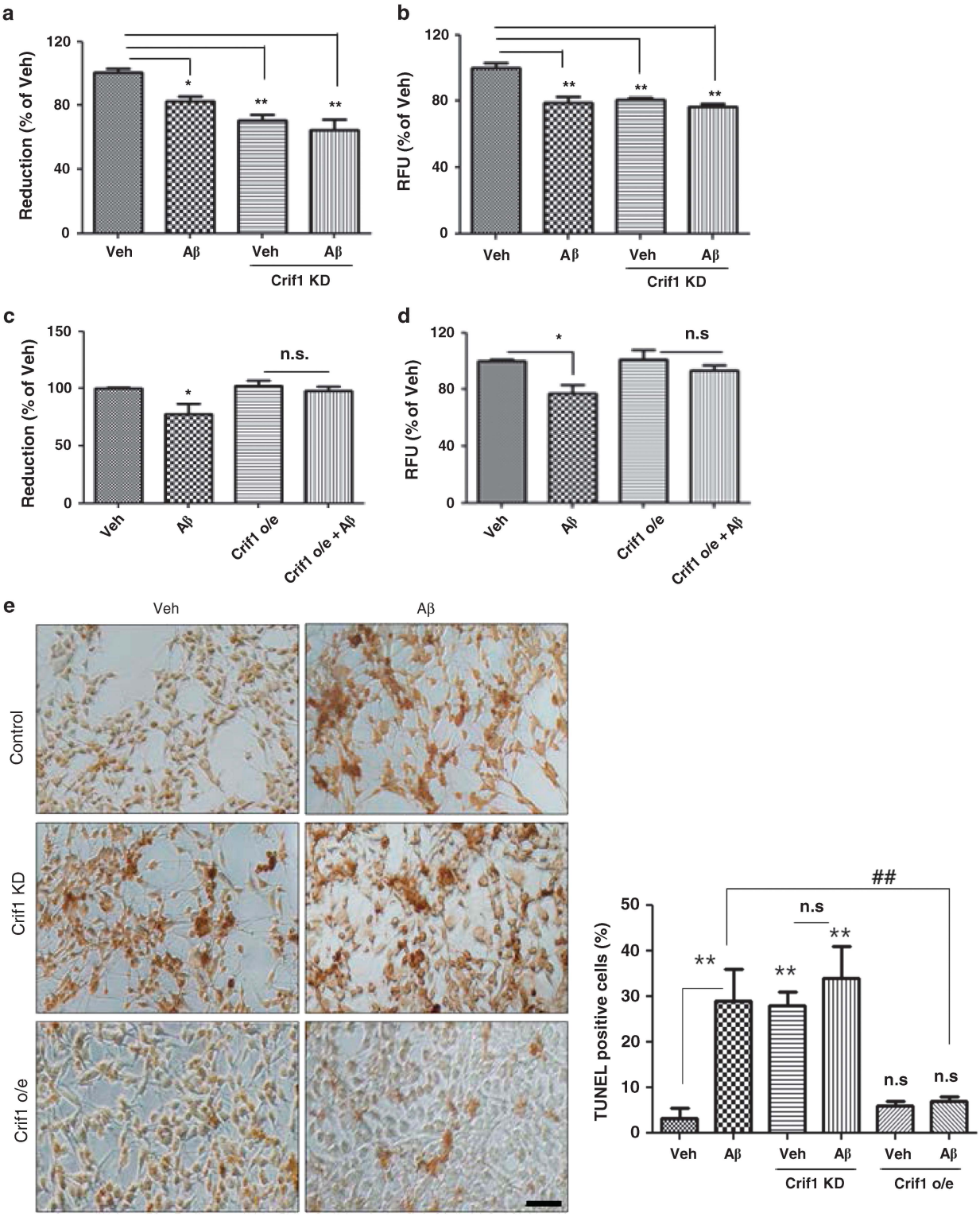

Figure 6 Crif1 levels are important for Aβ-induced cell death in SH-SY5Y cells. (**a** and **b**) Crif1 KD induced cell death by MTT assay (**a**) and Calcein-AM assay (**b**). Cell viability assays showed that Crif1 KD enhanced cell death as much as Aβ-treated condition (5 μM, 24 h). *$P<0.05$, **$P<0.01$ *versus* vehicle-treated control siRNA-transfected cells (**c** and **d**) Increased Crif1 expression blocked Aβ-induced cell death. After cDNA transfection for 24 h, 5 μM Aβ was administered for 24 h, and then MTT (**c**) and Calcein-AM assay (**d**) were performed. *$P<0.05$ *versus* vehicle-treated mock vector-transfected cells. Data were obtained from at least five replicates per group ($N=5$ experiments). (**e**) To confirm cell death in Crif1 KD or Crif1 o/e cells, TUNEL assay was performed. Scale bar represents 20 μm. Data are shown as mean $\pm$ S.E.M. of three independent experiments ($n=200$ each groups, $N=3$ experiments). **$P<0.01$ *versus* vehicle-treated mock vector-transfected cells; $^{\#\#}P<0.01$ *versus* Aβ-treated mock vector-transfected cells; NS indicates no significant difference

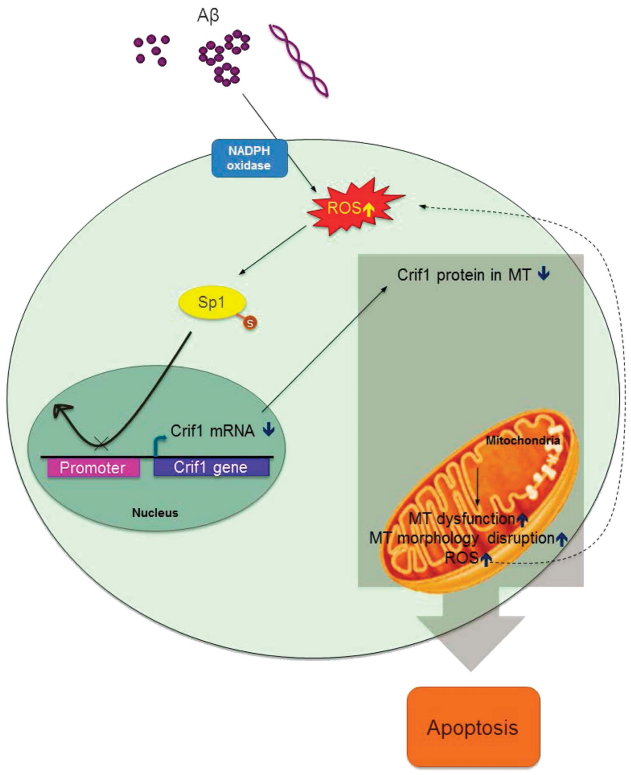

Figure 7 Schematic diagram for Aβ-induced mitochondrial dysfunction via ROS-Sp1-Crif1 pathway. Based on our experimental data, Aβ-induced ROS facilitated the reduction of Crif1 mRNA levels by increasing the sumoylation of Sp1. Reduced Crif1 expression resulted in disruption of mitochondrial morphology and mitochondrial functions, which leads to neuronal cell death shown in AD brains

Images were taken on a confocal laser scanning microscope (FV10i-w, Olympus, Tokyo, Japan) and quantified using the Image J program (NIH, Bethesda, MD, USA). To check for changes in mitochondrial morphology in detail, we used super-resolution structured illumination microscopy (SIM; Nikon N-SIM). Briefly, a 3D-SIM image of fixed cells was taken by moving the stage in the z-direction with a optimal step size (0.150 μm). Images were taken by Eclipse Ti-E research inverted microscope with Nikon's legendary CFI Apo TIRF ×100 oil objective lens (NA 1.49) and 512×512 pixel resolution with iXon DU-897 EMCCD camera (Andor Technology, South Windsor, CT, USA).

Mitochondrial function analysis. To measure MMP, TMRM and JC-1 assays were performed. TMRM assay was conducted as previously described. [5] For the JC-1 assay, we measured green to red ratio after treatment with JC-1 dye (2 μM). ATP measurements were conducted as previously described.[5] ROS levels were determined using dichloro-dihydrofluoresceindiacetate (Invitrogen) as previously described.[5] Mitochondria-specific ROS were measured using MitoSOX Red (5 mM for 15 min at 37 °C) following the manufacturer's instructions (Invitrogen). For all mitochondrial assays, cells were incubated for 24 h after the transfection of control and Crif1 siRNA or scrambled and Crif1 cDNA. Then, 5 μM Aβ was administered to cells for 24 h before performing the assays.

Cell viability assay. To measure cell viability, we performed Calcein-AM and MTT assays as previously described.[5] TUNEL assay was performed using the Deadend Colorimetric TUNEL System (Promega, Madison, WI, USA) according to the manufacturer's protocol. To analyze the TUNEL assay results, similar cell numbers from each group were analyzed ($n=200$). Data are represented as the mean ± S.E.M. from three independent experiments. For all cell death assays, cells were transfected with control and Crif1 siRNA or scrambled and Crif1 cDNA for 24 h and 5 μM Aβ was administered to cells for 24 h before the assay.

RNA isolation and reverse transcription-PCR. To measure Crif1 mRNA in SH-SY5Y cells, RNA was isolated using the RNeasyPlus Mini Kit (Qiagen, Valencia, CA, USA) and reverse transcription of the isolated RNA was performed in vehicle or 5 μM Aβ-treated SH-SY5Y cells. The following sense and antisense primers were used for human Crif1: 5′-GACAGGCACGC AGCCTACTA-3′ (sense), 5′-ATCATCTGTGGCATCTTGGC-3′ (antisense).

Quantitative real-time PCR. To examine the levels of mRNA of Crif1 or mitochondrial protein in human brain samples and SH-SY5Y cells, qRT-PCR was performed as previously described.[57] The following sense and antisense primers were used: 5′-GATGCCACAGATGATTGTGA-3′ (sense), 5′-CCGTTTCTGTTT TCCTCTCCT-3′ (antisense) for Crif1; 5′-CGACCGCAAAAGACGAAGTGAC-3′ (sense), 5′-GCTTCAGCATCTTTAAGGTCAGG-3′ (antisense) for TOM20; 5′-AGCA CTATGCCCTGGAGGATGA-3′ (sense), 5′-GAGCCAAGGAAGAGGTTCTGCT-3′ (antisense) for TIM50; 5′-ACAGCCGCATCTTCTTGTGCAGTG-3′(sense), 5′-GGCC TTGACTGTGCCGTTGAATTT-3′ (antisense) for GAPDH.

Electrophoretic mobility shift assay. To examine the interaction with the promoter region of Crif1 and Sp1 transcription factor, we performed an EMSA in vehicle or 5 μM Aβ-treated SH-SY5Y cells for 24 h using the Light Shift Chemiluminescent EMSA kit (Thermo Scientific, Hudson, NH, USA) following the manufacturer's protocol. A double-stranded probe was generated by annealing two biotin-labeled oligonucleotides against the putative Sp1-binding site (5′-ACCCGCCCC-3′) within the human Crif1 gene promoter region; forward probe (5′-biotin-TTTAATCGACCCG CCCCACC-3′) and reverse probe (5′-biotin-GGTG GGGCGGGTCGATTAAA-3′).

Co-immunoprecipitation. For Co-IP experiments, vehicle or SH-SY5Y cells treated with Aβ for 24 h were lysed with M-PER mammalian protein extraction reagent (Thermo Scientific) and processed as previously described.[58]

Immunostaining. Immunocytochemical staining was performed as previously described.[55] Images were obtained using a confocal laser scanning microscope (FV10i-w, Olympus). For histological analyses, Tg6799 mice were killed at 6 months of age ($n=6$ per group), brains were sliced and were stained for Crif1 (Santa Cruz Biotechnology; 1 : 250).[40] Immunohistochemistry on human brain tissues was performed as previously described.[59] Briefly, postmortem tissue blocks were cut into 40 μm-serial sections on a freezing sliding microtome (Model 860; American Optical Company, Buffalo, NY, USA). Sections were stored in cryoprotectant solution (30% glycerol, 30% ethylene glycol, 0.1% sodiumazide in PB; pH 7.4) at − 20 °C. Tissue sections were incubated for 48 h with anti-Crif1 (Santa Cruz Biotechnology; 1 : 100), then the sections were incubated in biotinylated horse anti-mouse IgG antibody (Vector Laboratories, Burlingame, CA, USA; 1 : 500) for 2 h at room temperature. Subsequently, the sections were incubated with streptavidin (Invitrogen; 1 : 5000) for 2 h at room temperature. Nickel-enhanced DAB/peroxidase reaction (0.02% DAB (Sigma-Aldrich), 0.08% nickel-sulfate, 0.006% hydrogen peroxide) was used to visualize the reaction product.

Aβ_{1-42} preparation. Aβ_{1-42} peptide (American peptide, Sunnyvale, CA, USA) was prepared as previously described.[55] Aβ_{1-42} peptide was dissolved in 1,1,1,3,3,3-hexafluoro-2-propanol (Sigma-Aldrich) to a concentration of 1 mM. The solution was aliquoted and 1,1,1,3,3,3-hexafluoro-2-propanol was evaporated by vacuum (SpeedVac Concentrator; Savant Instruments, Hyderabad, India). The dry peptide was maintained at − 80 °C and dissolved with anhydrous dimethyl sulfoxide to 1 mM following dilution in Opti-MEM (Invitrogen). Most of Aβ consisted predominantly of oligomers, and some monomers.[56]

Statistical analysis. For WB, protein levels were normalized to pan forms or a housekeeping protein, such as β-actin or GAPDH. All data were expressed as means ± standard error of the mean (S.E.M.). Student's *t*-test was used for two-group comparisons, and analysis of variance, followed by Fisher's LSD *post-hoc* test, was used to compare three or more groups using SigmaStat for Windows Version 3.10 (Systat Software, Inc., Point Richmond, CA, USA). *P* values <0.05 were considered statistically significant.

Conflict of Interest

The authors declare no conflict of interest.

Acknowledgements. This work was supported by grants from NRF (2012R1A2A1A01002881, 2014M3C7A1046047, MRC (2011-0030738)), KNIH ROAD R&D Program Project (A092058) to IM-J. AD tissues were provided by the Harvard Brain Tissue Resource Center of McLean Hospital.

Author contributions

JB and SMS performed research, collected data, and wrote the manuscript. YJH, YK, HR, MM and K-SK performed research and collected data for human brain tissues. M-YC, MS and SKP collected data. IM-J supervised the study and reviewed and edited the manuscript.

1. Katzman R. Alzheimer's disease. *N Engl J Med* 1986; **314**: 964–973.
2. Walsh DM, Selkoe DJ. Deciphering the molecular basis of memory failure in Alzheimer's disease. *Neuron* 2004; **44**: 181–193.
3. Querfurth HW, LaFerla FM. Alzheimer's disease. *N Engl J Med* 2010; **362**: 329–344.
4. Baloyannis SJ, Costa V, Michmizos D. Mitochondrial alterations in Alzheimer's disease. *Am J Alzheimers Dis Other Demen* 2004; **19**: 89–93.
5. Cha MY, Han SH, Son SM, Hong HS, Choi YJ, Byun J *et al.* Mitochondria-specific accumulation of amyloid beta induces mitochondrial dysfunction leading to apoptotic cell death. *PLoS One* 2012; **7**: e34929.
6. Lin MT, Beal MF. Mitochondrial dysfunction and oxidative stress in neurodegenerative diseases. *Nature* 2006; **443**: 787–795.
7. Chacinska A, Koehler CM, Milenkovic D, Lithgow T, Pfanner N. Importing mitochondrial proteins: machineries and mechanisms. *Cell* 2009; **138**: 628–644.
8. Youle RJ, Karbowski M. Mitochondrial fission in apoptosis. *Nat Rev Mol Cell Biol* 2005; **6**: 657–663.
9. Knott AB, Perkins G, Schwarzenbacher R, Bossy-Wetzel E.. Mitochondrial fragmentation in neurodegeneration. *Nat Rev Neurosci* 2008; **9**: 505–518.
10. Wang X, Su B, Siedlak SL, Moreira PI, Fujioka H, Wang Y *et al.* Amyloid-beta overproduction causes abnormal mitochondrial dynamics via differential modulation of mitochondrial fission/fusion proteins. *Proc Natl Acad Sci USA* 2008; **105**: 19318–19323.
11. Perry G, Nunomura A, Hirai K, Zhu X, Prez M, Avila J *et al.* Is oxidative damage the fundamental pathogenic mechanism of Alzheimer's and other neurodegenerative diseases? *Free Radic Biol Med* 2002; **33**: 1475–1479.
12. de la Monte SM, Luong T, Neely TR, Robinson D, Wands JR. Mitochondrial DNA damage as a mechanism of cell loss in Alzheimer's disease. *Lab Invest* 2000; **80**: 1323–1335.
13. Oh NS, Yoon SH, Lee WK, Choi JY, Min do S, Bae YS. Phosphorylation of CKBBP2/CRIF1 by protein kinase CKII promotes cell proliferation. *Gene* 2007; **386**: 147–153.
14. Zhang X, Ran Q, Li Z, Liu Y, Liang X, Chen X. Cell cycle arrest of Jurkat cells by leukemic bone marrow stromal cells: possible mechanisms and involvement of CRIF1. *Transplant Proc* 2011; **43**: 2770–2773.
15. Kang HJ, Hong YB, Kim HJ, Bae I. CR6-interacting factor 1 (CRIF1) regulates NF-E2-related factor 2 (NRF2) protein stability by proteasome-mediated degradation. *J Biol Chem* 2010; **285**: 21258–21268.
16. Kim SJ, Kwon MC, Ryu MJ, Chung HK, Tadi S, Kim YK *et al.* CRIF1 is essential for the synthesis and insertion of oxidative phosphorylation polypeptides in the mammalian mitochondrial membrane. *Cell Metab* 2012; **16**: 274–283.
17. Son SM, Jung ES, Shin HJ, Byun J, Mook-Jung I. Abeta-induced formation of autophagosomes is mediated by RAGE-CaMKKbeta-AMPK signaling. *Neurobiol Aging* 2012; **33**: 1006 e1011–1006 e1023.
18. Lee DH, Goldberg AL. Proteasome inhibitors: valuable new tools for cell biologists. *Trends Cell Biol* 1998; **8**: 397–403.
19. Klionsky DJ, Abdalla FC, Abeliovich H, Abraham RT, Acevedo-Arozena A, Adeli K *et al.* Guidelines for the use and interpretation of assays for monitoring autophagy. *Autophagy* 2012; **8**: 445–544.
20. Zorov DB, Juhaszova M, Sollott SJ. Mitochondrial ROS-induced ROS release: an update and review. *Biochim Biophys Acta* 2006; **1757**: 509–517.
21. Shelat PB, Chalimoniuk M, Wang JH, Strosznajder JB, Lee JC, Sun AY *et al.* Amyloid beta peptide and NMDA induce ROS from NADPH oxidase and AA release from cytosolic phospholipase A2 in cortical neurons. *J Neurochem* 2008; **106**: 45–55.
22. t Hart BA, Simons JM, Knaan-Shanzer S, Bakker NP, Labadie RP. Antiarthritic activity of the newly developed neutrophil oxidative burst antagonist apocynin. *Free Radic Biol Med* 1990; **9**: 127–131.
23. Cross AR, Jones OT. The effect of the inhibitor diphenylene iodonium on the superoxide-generating system of neutrophils. Specific labelling of a component polypeptide of the oxidase. *Biochem J* 1986; **237**: 111–116.
24. Sang J, Yang K, Sun Y, Han Y, Cang H, Chen Y *et al.* SUMO2 and SUMO3 transcription is differentially regulated by oxidative stress in an Sp1-dependent manner. *Biochem J* 2011; **435**: 489–498.
25. Hsin IL, Sheu GT, Chen HH, Chiu LY, Wang HD, Chan HW *et al.* N-acetyl cysteine mitigates curcumin-mediated telomerase inhibition through rescuing of Sp1 reduction in A549 cells. *Mutat Res* 2010; **688**: 72–77.
26. Spengler ML, Brattain MG. Sumoylation inhibits cleavage of Sp1 N-terminal negative regulatory domain and inhibits Sp1-dependent transcription. *J Biol Chem* 2006; **281**: 5567–5574.
27. Wang YT, Yang WB, Chang WC, Hung JJ. Interplay of posttranslational modifications in Sp1 mediates Sp1 stability during cell cycle progression. *J Mol Biol* 2011; **414**: 1–14.
28. Knott AB, Perkins G, Schwarzenbacher R, Bossy-Wetzel E. Mitochondrial fragmentation in neurodegeneration. *Nat Rev Neurosci* 2008; **9**: 505–518.
29. Tillement L, Lecanu L, Papadopoulos V. Alzheimer's disease: Effects of β-amyloid on mitochondria. *Mitochondrion* 2011; **11**: 13–21.
30. Youle RJ, Karbowski M. Mitochondrial fission in apoptosis. *Nat Rev Mol Cell Biol* 2005; **6**: 657–663.
31. Aliev G, Smith MA, de la Torre JC, Perry G. Mitochondria as a primary target for vascular hypoperfusion and oxidative stress in Alzheimer's disease. *Mitochondrion* 2004; **4**: 649–663.
32. Wang X, Su B, Siedlak SL, Moreira PI, Fujioka H, Wang Y *et al.* Amyloid-β overproduction causes abnormal mitochondrial dynamics via differential modulation of mitochondrial fission/fusion proteins. *Proc Natl Acad Sci* 2008; **105**: 19318–19323.
33. Darshi M, Mendiola VL, Mackey MR, Murphy AN, Koller A, Perkins GA *et al.* ChChd3, an inner mitochondrial membrane protein, is essential for maintaining crista integrity and mitochondrial function. *J Biol Chem* 2011; **286**: 2918–2932.
34. Alkhaja AK, Jans DC, Nikolov M, Vukotic M, Lytovchenko O, Ludewig F *et al.* MINOS1 is a conserved component of mitofilin complexes and required for mitochondrial function and cristae organization. *Mol Biol Cell* 2012; **23**: 247–257.
35. Merkwirth C, Langer T. Prohibitin function within mitochondria: essential roles for cell proliferation and cristae morphogenesis. *Biochim Biophys Acta* 2009; **1793**: 27–32.
36. NUNOMURA A, PERRY G, ALIEV G, HIRAI K, TAKEDA A, BALRAJ EK *et al.* Oxidative Damage Is the Earliest Event in Alzheimer Disease. *J Neuropathol Exp Neurol* 2001; **60**: 759–767.
37. Resende R, Moreira PI, Proença T, Deshpande A, Busciglio J, Pereira C *et al.* Brain oxidative stress in a triple-transgenic mouse model of Alzheimer disease. *Free Radic Biol Med* 2008; **44**: 2051–2057.
38. Ryu H, Lee J, Zaman K, Kubilis J, Ferrante RJ, Ross BD *et al.* Sp1 and Sp3 are oxidative stress-inducible, antideath transcription factors in cortical neurons. *J Neurosci* 2003; **23**: 3597–3606.
39. Citron BA, Dennis JS, Zeitlin RS, Echeverria V. Transcription factor Sp1 dysregulation in Alzheimer's disease. *J Neurosci Res* 2008; **86**: 2499–2504.
40. Cho HJ, Son SM, Jin SM, Hong HS, Shin DH, Kim SJ *et al.* RAGE regulates BACE1 and Abeta generation via NFAT1 activation in Alzheimer's disease animal model. *FASEB J* 2009; **23**: 2639–2649.
41. Xie H, Hou S, Jiang J, Sekutowicz M, Kelly J, Bacskai BJ. Rapid cell death is preceded by amyloid plaque-mediated oxidative stress. *Proc Natl Acad Sci USA* 2013; **110**: 7904–7909.
42. Oakley H, Cole SL, Logan S, Maus E, Shao P, Craft J *et al.* Intraneuronal beta-amyloid aggregates, neurodegeneration, and neuron loss in transgenic mice with five familial Alzheimer's disease mutations: potential factors in amyloid plaque formation. *J Neurosci* 2006; **26**: 10129–10140.
43. Rojas S, Herance JR, Gispert JD, Abad S, Torrent E, Jimenez X *et al.* In vivo evaluation of amyloid deposition and brain glucose metabolism of 5XFAD mice using positron emission tomography. *Neurobiol Aging* 2013; **34**: 1790–1798.
44. Du H, Guo L, Fang F, Chen D, Sosunov AA, McKhann GM *et al.* Cyclophilin D deficiency attenuates mitochondrial and neuronal perturbation and ameliorates learning and memory in Alzheimer's disease. *Nat Med* 2008; **14**: 1097–1105.
45. Schmidt C, Lepsverdize E, Chi SL, Das AM, Pizzo SV, Dityatev A *et al.* Amyloid precursor protein and amyloid beta-peptide bind to ATP synthase and regulate its activity at the surface of neural cells. *Mol Psychiatry* 2008; **13**: 953–969.
46. Hansson Petersen CA, Alikhani N, Behbahani H, Wiehager B, Pavlov PF, Alafuzoff I *et al.* The amyloid beta-peptide is imported into mitochondria via the TOM import machinery and localized to mitochondrial cristae. *Proc Natl Acad Sci USA* 2008; **105**: 13145–13150.
47. Cali T, Ottolini D, Brini M. Mitochondrial Ca(2+) and neurodegeneration. *Cell Calcium* 2012; **52**: 73–85.
48. Kannurpatti SS, Biswal BB. Mitochondrial Ca2+ uniporter blockers influence activation-induced CBF response in the rat somatosensory cortex. *J Cereb Blood Flow Metab* 2008; **28**: 772–785.
49. Paumard P, Vaillier J, Coulary B, Schaeffer J, Soubannier V, Mueller DM *et al.* The ATP synthase is involved in generating mitochondrial cristae morphology. *EMBO J* 2002; **21**: 221–230.
50. Goyon V, Fronzes R, Salin B, di-Rago JP, Velours J, Brethes D. Yeast cells depleted in Atp14p fail to assemble Atp6p within the ATP synthase and exhibit altered mitochondrial cristae morphology. *J Biol Chem* 2008; **283**: 9749–9758.
51. Schleicher M, Shepherd BR, Suarez Y, Fernandez-Hernando C, Yu J, Pan Y *et al.* Prohibitin-1 maintains the angiogenic capacity of endothelial cells by regulating mitochondrial function and senescence. *J Cell Biol* 2008; **180**: 101–112.
52. Hsiao K, Chapman P, Nilsen S, Eckman C, Harigaya Y, Younkin S *et al.* Correlative memory deficits, Abeta elevation, and amyloid plaques in transgenic mice. *Science* 1996; **274**: 99–102.
53. Jankowsky JL, Fadale DJ, Anderson J, Xu GM, Gonzales V, Jenkins NA *et al.* Mutant presenilins specifically elevate the levels of the 42 residue beta-amyloid peptide *in vivo*: evidence for augmentation of a 42-specific gamma secretase. *Hum Mol Genetics* 2004; **13**: 159–170.
54. Oakley H, Cole SL, Logan S, Maus E, Shao P, Craft J *et al.* Intraneuronal beta-amyloid aggregates, neurodegeneration, and neuron loss in transgenic mice with five familial

Alzheimer's disease mutations: potential factors in amyloid plaque formation. *J Neurosci* 2006; **26**: 10129–10140.
55. Son SM, Song H, Byun J, Park KS, Jang HC, Park YJ *et al.* Altered APP processing in insulin-resistant conditions is mediated by autophagosome accumulation via the inhibition of mammalian target of rapamycin pathway. *Diabetes* 2012; **61**: 3126–3138.
56. Moon M, Hong HS, Nam DW, Baik SH, Song H, Kook SY *et al.* Intracellular amyloid-beta accumulation in calcium-binding protein-deficient neurons leads to amyloid-beta plaque formation in animal model of Alzheimer's disease. *J Alzheimers Dis* 2012; **29**: 615–628.
57. Lee J, Hwang YJ, Shin JY, Lee WC, Wie J, Kim KY *et al.* Epigenetic regulation of cholinergic receptor M1 (CHRM1) by histone H3K9me3 impairs Ca(2+) signaling in Huntington's disease. *Acta Neuropathol* 2013; **125**: 727–739.
58. Son SM, Byun J, Roh SE, Kim SJ, Mook-Jung I. Reduced IRE1alpha mediates apoptotic cell death by disrupting calcium homeostasis via the InsP3 receptor. *Cell Death Dis* 2014; **5**: e1188.
59. Pantazopoulos H, Boyer-Boiteau A, Holbrook EH, Jang W, Hahn CG, Arnold SE *et al.* Proteoglycan abnormalities in olfactory epithelium tissue from subjects diagnosed with schizophrenia. *Schizophr Res* 2013; **150**: 366–372.

Supplementary Information accompanies this paper on Cell Death and Differentiation website (http://www.nature.com/cdd)